THE STRUCTURAL DESIGN OF TALL AND SPECIAL BUILDINGS
Struct. Design Tall Spec. Build. **18**, 351–370 (2009)
Published online 19 November 2007 in Wiley Interscience (www.interscience.wiley.com). **DOI**: 10.1002/tal.420

SEISMIC PERFORMANCE OF TUBULAR STRUCTURES WITH BUCKLING RESTRAINED BRACES

JINKOO KIM[1]*, JUNHEE PARK[1], SUNG-WOO SHIN[2] AND KYUNG-WON MIN[3]
[1] *Department of Architectural Engineering, Sungkyunkwan University, Suwon, Korea*
[2] *Department of Architectural Engineering, Hangyang University, Ansan, Korea*
[3] *Department of Architectural Engineering, Dankook University, Sungnam, Korea*

SUMMARY

In this study 36- and 72-story framed and braced tubular structures were designed according to the current design code and their seismic performances were evaluated by nonlinear static and dynamic analysis. According to the analysis results, the tubular structures generally showed high earthquake-resisting capability. The framed tube structure showed lowest stiffness and strength compared with the other model structures. The braced tube structures showed larger strength but lower overall ductility compared with framed tube structures. When buckling-restrained braces were used instead of conventional braces, strength increased significantly compared with the framed tube, and ductility was enhanced compared with braced tube structures. As the load–displacement relationship estimated by static pushover analysis formed the lower bound of the dynamic analysis results, the response modification factors obtained based on the static pushover curve may safely be used for seismic design. Copyright © 2007 John Wiley & Sons, Ltd.

1. INTRODUCTION

Tubular structures have been widely used as an efficient structural system for tall buildings. Typical tube systems are composed of perimeter moment-resisting frames which resist all the lateral loads and internal frames supporting only gravity loads. The tubular behavior allows considerable freedom in architectural planning of the interior space. Many super-tall buildings, including the 110-story Sears Tower and the 100-story John Hancock Building in Chicago, were built using tubular systems.

Idealized tubular structures behave as a hollow tube responding predominantly in a bending mode. Tubular behavior is achieved by placing external columns 1·0–3·0 m to as much as 6 m apart, with depth of spandrel girders varying from 1·0 to 1·5 m (Taranath, 1998). Further improvement in stiffness and strength can be obtained by employing diagonal members in the exterior moment frames to induce truss action in the perimeter of the structure. Sometimes the same effect as diagonal bracing can be achieved by infilling window penetrations in a systematic pattern. Another version of enhancing tubular action is to use many tubes tied together to form a bundled tube.

Previous research on tubular structures generally focused on wind-induced responses (Connor and Pouangaree, 1992; Koran, 1994), and research on inelastic seismic performance is relatively rare. This is attributed to the common preconception that tall buildings are not vulnerable to seismic load because their fundamental natural period is significantly long enough to remain away from the acceleration-

*Correspondence to: Jinkoo Kim, Department of Architectural Engineering, Sungkyunkwan University, Cheoncheon-dong, Jangan-gu, Suwon-si, Gyeonggi-do 440-746, Republic of Korea. E-mail: jkim12@skku.edu

sensitive region of response spectra. However, the design seismic load level in the United States has generally increased from 10/50 events (10% probability of occurrence in 50 years) to two-thirds of 2/50 events. Also the current trend of seismic engineering is to recommend that structural responses for various levels of seismic ground motion be checked; the guideline for performance-based seismic engineering (FEMA-356) requires that the structure be designed to satisfy a collapse prevention limit state for 2/50 seismic events. In this sense it would be necessary to evaluate the seismic performance of tall buildings for large seismic events exceeding design seismic load level to ensure the safety of occupants.

In this paper 36- and 72-story framed and braced tubular structures were designed and their seismic performance was evaluated using nonlinear static and dynamic analyses. Also the effectiveness of using buckling restrained braces (BRBs) instead of normal braces was investigated.

2. DESIGN OF ANALYSIS MODEL STRUCTURES

The basic configuration of a tubular structure is a box-type structure, so that it can resist lateral loads, like the hollow box tube depicted schematically in Figure 1. The analysis models are 36-story and 72-story framed tube structures (FTS) and braced tube structures (BTS). For comparison, other braced tube structures with buckling-restrained braces (BRB) were prepared. Figure 2 plots the structural plan and side view of the 36-story tubular structures. The structures are 36 m × 36 m in plan and the story height is 3·6 m. The spacings of external columns are 3 m and 6 m for the framed and braced tube structures, respectively. The pin-connected internal frames were designed only for gravity load, which is composed of a dead load of 4 kN/m^2 and a live load of 2·5 kN/m^2. The design seismic load was computed using the design spectrum of the International Building Code (ICC, 2006) with $S_{DS} = 0{\cdot}29$ and $S_{D1} = 0{\cdot}12$. A response modification factor (*R*-factor) of 3·0 was used for both model structures, considering that tubular structures are not defined as one of the basic seismic force-resisting systems. Although the value used is smaller than the *R*-factor of ordinary steel moment-resisting frames, which is 4·0, the value seems to be reasonable considering the fact that the failure mode of tubular structures

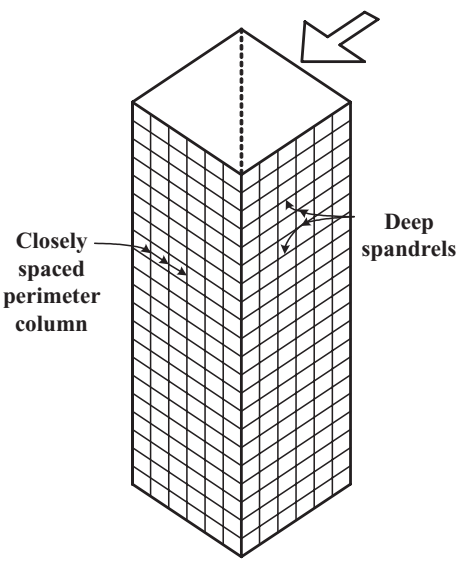

Figure 1. Schematic of tubular structures (Taranath, 1998)

DOI: 10.1002/tal

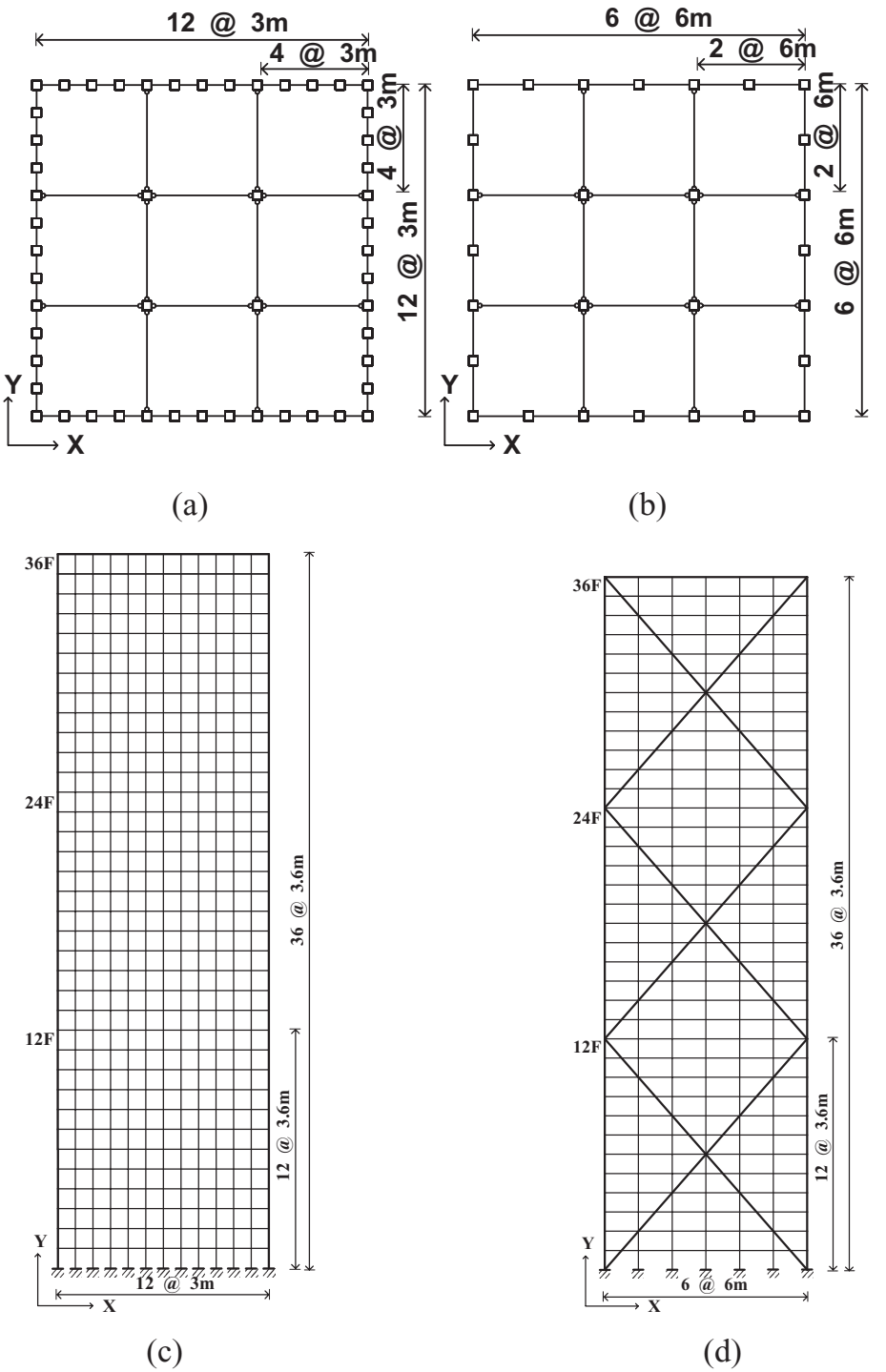

Figure 2. 36-story tubular structure analysis models: (a) structural plan (framed tube); (b) structural plan (braced tube); (c) elevation of framed tube; (d) elevation of braced tube

DOI: 10.1002/tal

may be associated with buckling of external columns and therefore with brittle failure mode. The design wind load was computed using a basic wind speed of 30 m/s at exposure category A. Figure 3 compares the design seismic and wind loads imposed on the model structures, where it can be observed that the base shears induced by the wind load are significantly larger than those of the seismic load. The design and nonlinear static analysis of the model structures were carried out using the general-purpose finite element program code MIDAS (2007), and SAP 2000 was used for nonlinear dynamic analysis. The structural member design was carried out in accordance with the AISC LRFD (2000), and the same members were used in three consecutive stories. Figure 4 shows the lateral displacements of the framed tube model structures subjected to design wind and seismic loads. It can be observed that the story drifts for the wind load are larger than those for the seismic load. In the 36-story FTS the maximum displacement is significantly smaller than the drift criterion (1/500 of the building height). The wind-induced maximum displacements of all the 72-story model structures designed for strength far exceeded the drift criterion, and they were redesigned to meet the criterion. Table 1 summarizes the size of the selected members of the FTS and BTS model structures. The yield stresses of the columns/braces and beams are 330 MPa and 240 MPa, respectively, and the ultimate strengths are 490 MPa and 400 MPa, respectively.

BRB consist of a steel core capable of undergoing significant inelastic deformation and a casing for restraining global and local buckling of the core element, as shown in Figure 5. According to previous research, a BRB exhibits stable hysteretic behavior with superb energy dissipation capacity. Tremblay *et al.* (1999) conducted a quasi-static loading test on BRB and showed that the strain-hardening behavior is most likely the result of Poisson's effects on the steel plate undergoing large inelastic deformation. Black *et al.* (2001) presented test results of five BRB with various configurations. Their study concluded that BRB is a reliable and practical alternative to conventional lateral load-resisting systems. Recently FEMA-450 (BSSC, 2004) and AISC (2005) Seismic Provisions provided regulations and design guidelines for BRB. The seismic provisions regulate the design strength of core elements as follows:

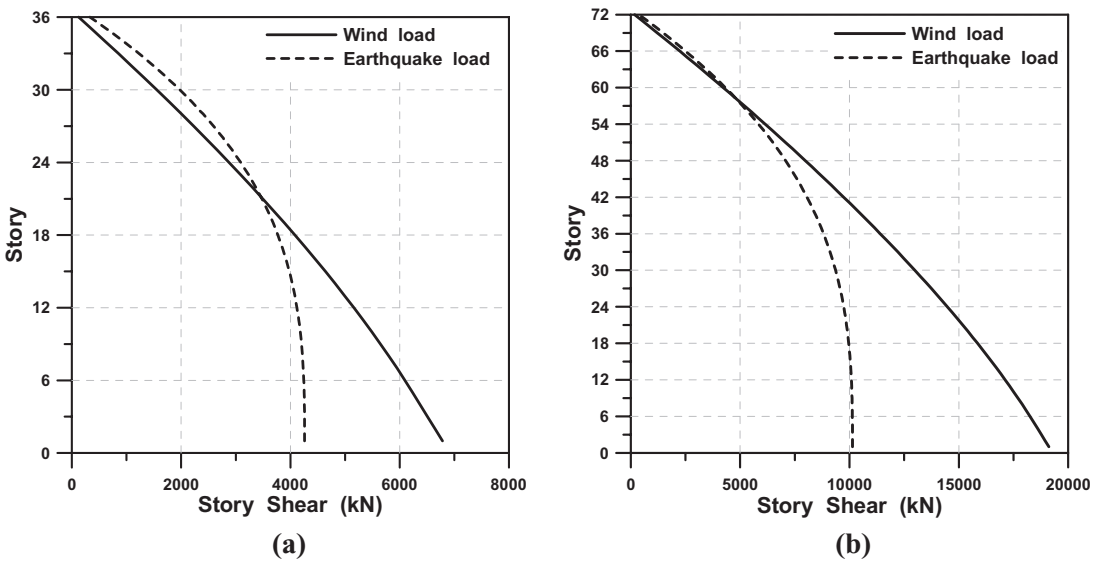

Figure 3. Comparison of design wind and seismic loads imposed on the framed tube model structures: (a) 36-story; (b) 72-story

DOI: 10.1002/tal

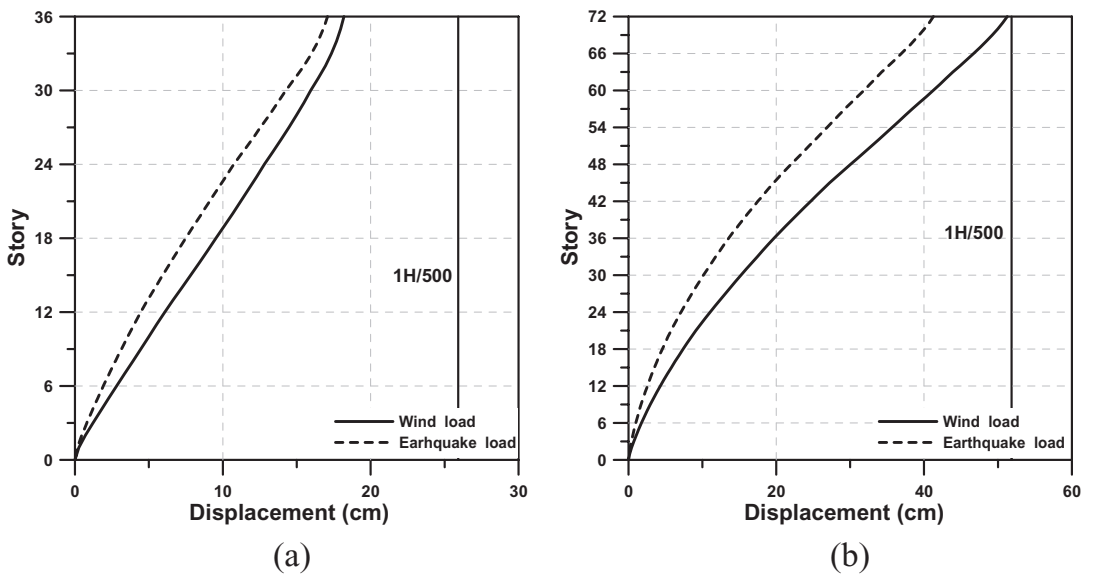

Figure 4. Lateral displacements of the framed tube structures subjected to design wind and seismic loads: (a) 36-story; (b) 72-story

Table 1. Selected members for 36-story analysis model structures (unit: MPa, mm)

(a) Framed tube system (FTS)				
Members	Ultimate strength	Stories	Size	Strength ratio
External columns	490	1–3	□ 450 × 300 × 22	0·99
		34–36	□ 300 × 300 × 10	0·77
Spandrel girders	400	1–3	*H* 800 × 300 × 20 × 23	0·41
		34–36	*H* 800 × 300 × 20 × 20	0·25
(b) Braced tube system (BTS)				
Members	Ultimate strength	Stories	Size	Strength ratio
External columns	490	1–3	□ 500 × 450 × 21	0·96
		34–36	□ 300 × 300 × 10	0·81
Spandrel girders	400	1–3	*H* 600 × 400 × 16 × 21	0·25
		34–36	*H* 500 × 300 × 16 × 21	0·27
Braces	490	1–3	□ 400 × 400 × 26	0·80
		34–36	□ 300 × 300 × 10	0·60

$$P_{nsc} = \phi P_{ysc}; \quad \phi = 0.9 \tag{1}$$

$$P_{ysc} = F_y \times A_{sc} \tag{2}$$

where F_y is the yield strength and A_{sc} is the cross-sectional area of core elements. In this study braced tubes with BRB (BRBTS) were designed for the same design loads and the seismic behavior was compared with those of framed and braced tube structures.

DOI: 10.1002/tal

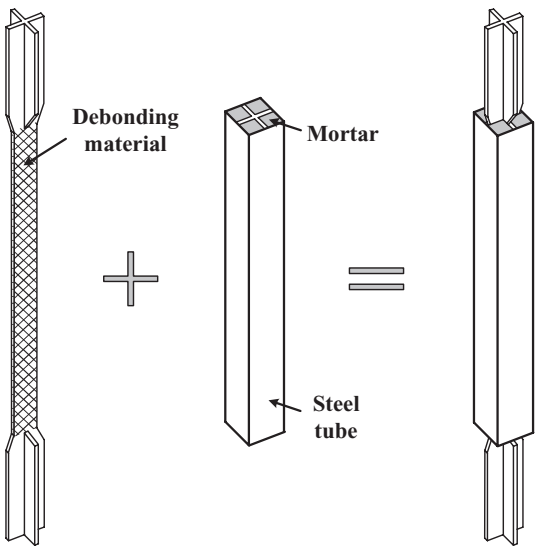

Figure 5. Typical buckling restrained brace

Table 2. Natural periods of analysis model structures

Analysis models	Natural periods (s)
36-FTS	3·92
36-BTS	2·99
36-BRBTS	3·14
72-FTS	5·55
72-BTS	5·34
72-BRBTS	5·35

Table 2 shows the natural periods of the model structures. In the 36-story model structures the natural period of the FTS is significantly larger than those of the braced tube systems. As the masses of model structures are almost identical, the difference in natural period results from the difference in stiffness. Therefore it can be expected that the FTS is very flexible compared with the other model structures. Since the core member of a BRB can sustain larger axial force in compression compared with conventional steel braces with the same cross-sectional area, smaller sections are selected for the same design load. This explains the slightly longer natural period of the BRBTS compared with that of the BTS. In the 72-story structures the natural periods of all model structures are similar, mainly because they were designed not for strength but for stiffness, to meet the drift criterion (1/500 of structure height).

3. NONLINEAR STATIC ANALYSIS OF MODEL STRUCTURES

For nonlinear analysis of braces the mathematical model presented in FEMA-356 was used. Figure 6 shows the axial load–deformation relationship of braces where F_y and P_{cr} represent the yield stress and the buckling strength, respectively, and Δ_y and A denote the axial yield displacement and the cross-sectional area of the brace. The post-buckling strength of braces P'_{cr} was taken as 20% of the buckling strength P_{cr}. Nonlinear static pushover analyses of the model structures were carried out by

DOI: 10.1002/tal

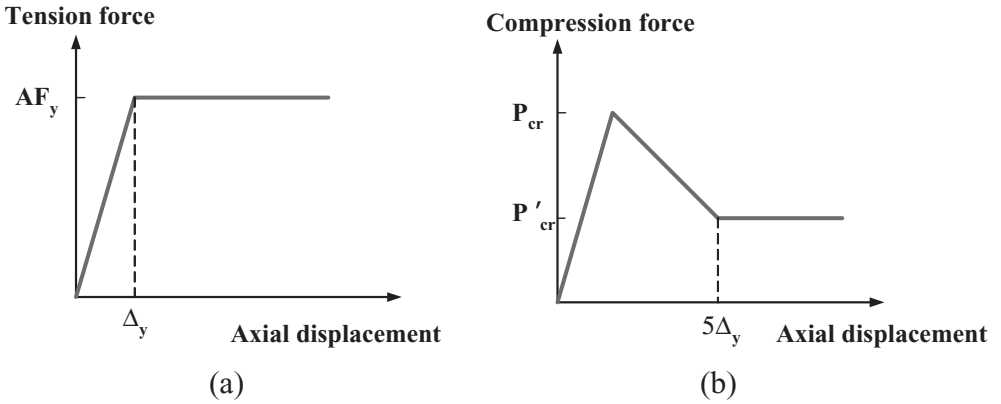

Figure 6. Force–displacement relationship of braces recommended in FEMA 356: (a) braces under tension; (b) braces under compression

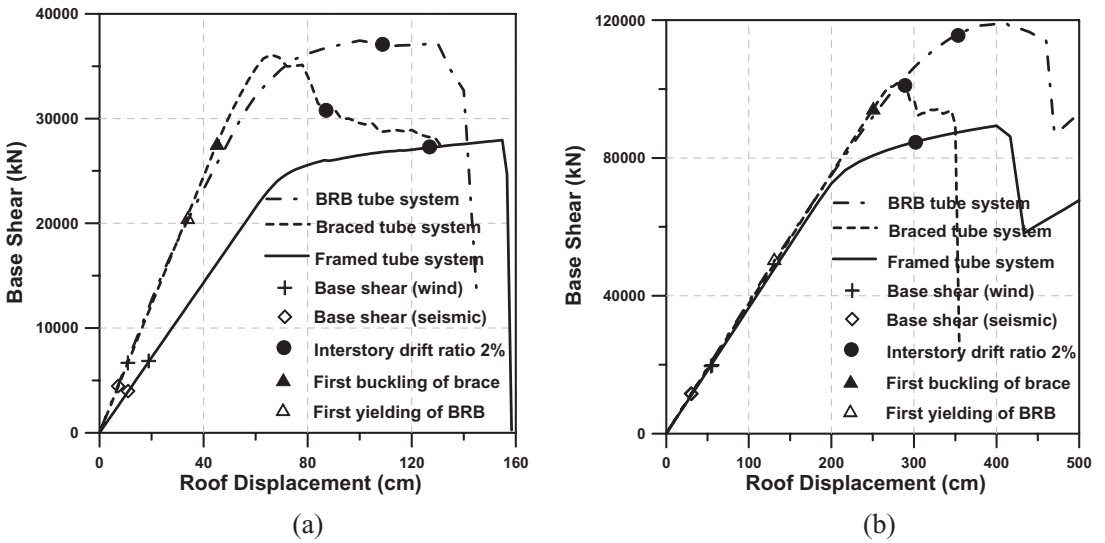

Figure 7. Pushover curves of the model structures: (a) 36-story structures; (b) 72-story structures

applying lateral load proportional to the following multi-mode story-wise distribution pattern, proposed by Freeman *et al.* (1998):

$$F_i = \sqrt{\sum_{j=1}^{N}\left\{\left(\frac{\sum_{k=1}^{N} m_k\phi_{kj}}{\sum_{k=1}^{N} m_k\phi_{kj}^2}\right)\phi_{ij}S_{aj}m_i\right\}^2} \tag{3}$$

where F_i and m_i are the seismic story force and story mass of the ith story, respectively; N is the number of stories; ϕ_{ij} is the ith component of the jth vibration mode; and S_{ij} is the pseudo-acceleration of the jth mode.

Figure 7 shows the load–displacement curves of the model structures. Indicated on the curves are the design base shears for earthquake and wind loads, the points of the first yield (BRBTS) or buckling

DOI: 10.1002/tal

of braces (BTS), and the points at which the maximum inter-story drift reached 2% of the story height, which is recommended as the collapse-prevention limit state in the FEMA-450 report (BSSC, 2004). According to the pushover analysis results, the stiffness and strength of the 36-story FTS turned out to be much smaller than those of the braced tube structures (BTS and BRBTS) with the same height. As mentioned above, smaller brace sections were selected in the BRBTS compared with BTS for give design loads. This results in slightly smaller initial stiffness (although not quite distinct in the figure). The stiffness of the BRBTS further decreased after the yielding of braces subjected to compression. After yielding the FTS behaved stably until the lateral load-resisting capacity of the structure was completely lost at the maximum inter-story drift of 3·4% of the story height. The failure point is much larger than the collapse-prevention limit state of the maximum inter-story drift of 2%. However, after the maximum strength was reached, the strength of the BTS dropped significantly before the limit state was reached as a result of buckling of braces and columns, while the behavior of BRBTS resembled that of the FTS, except that the stiffness and strength are much higher. In the 72-story structures the stiffnesses of all the model structures are almost identical because they were designed to meet the same drift criterion. The FTS showed large ductility, while the BTS showed brittle behavior with small ductility. It can be observed that immediatly after the first buckling of a brace the maximum strength of BTS was reached, followed by the collapse of the structure. On the contrary, the BRBTS showed relatively large maximum strength and ductility. Figure 8 depicts the plastic hinge formation in the web-side frame (parallel to the direction of lateral load) of the 36-story FTS. The empty and the filled circles denote that the members yielded or buckled by tension + flexure and compression + flexure, respectively. The size of the circle represents the magnitude of plastic deformation. It can be observed that some columns located in the third to sixth stories started to yield at the maximum inter-story drift (δ_1) of 0·52% (Figure 8a) due to the combined load of axial compression and bending moment. In the interaction equation to check the failure of the first story corner column, it was found that the contributions from the axial compression and bending moment were about 60% and 40%, respectively. The contribution of bending moment increased in columns located in higher stories. This shows that the columns located in the web-side frames of FTS are subjected to a significant amount of bending moment. As the lateral load increased the number of plastic hinges increased, and at the maximum inter-story drift of 2% the plastic hinges spread to all columns located in the fourth to seventh stories, as shown in Figure 8(c).

The distribution of plastic hinges and buckled members in the 36-story BTS is plotted in Figure 9. The empty and filled squares on braces represent the tension yield and the compression buckling (compression yielding in the BRBTS), respectively. It can be observed in Figure 9(a) that the first buckling occurred in a brace located in the seventh story at the maximum inter-story drift of 0·49%. When the maximum inter-story drift increased to 0·59%, more lower-story braces subjected to compression buckled and the corner columns in the 10th to 12th stories buckled (Figure 9b). The contribution of axial compression to the interaction equation was 93% in the first-story corner column, which is significantly higher than that of the FTS. Figure 9(c) shows the buckled or yielded members of the BTS in the 2% maximum inter-story drift. It can be observed that buckling or yielding occurred in many of the lower-story braces, columns and girders. As the inelastic deformation was concentrated in lower stories, overall ductility was quite limited. On the other hand, in the BRBTS the members with inelastic deformation spread to wider region of the exterior frame, as shown in Figure 10, which resulted in a significant increase in overall ductility.

Figure 11 presents the members with inelastic deformation in the flange-side (leeward) frame of the 36-story model structures. It was observed that in all model structures the corner columns located in lower stories buckled under compression. The contribution of compression to the interaction equation in FTS was about 80% of combined failure load. The contribution of axial compression in the braced tube structures was as high as 95% of combined failure load.

DOI: 10.1002/tal

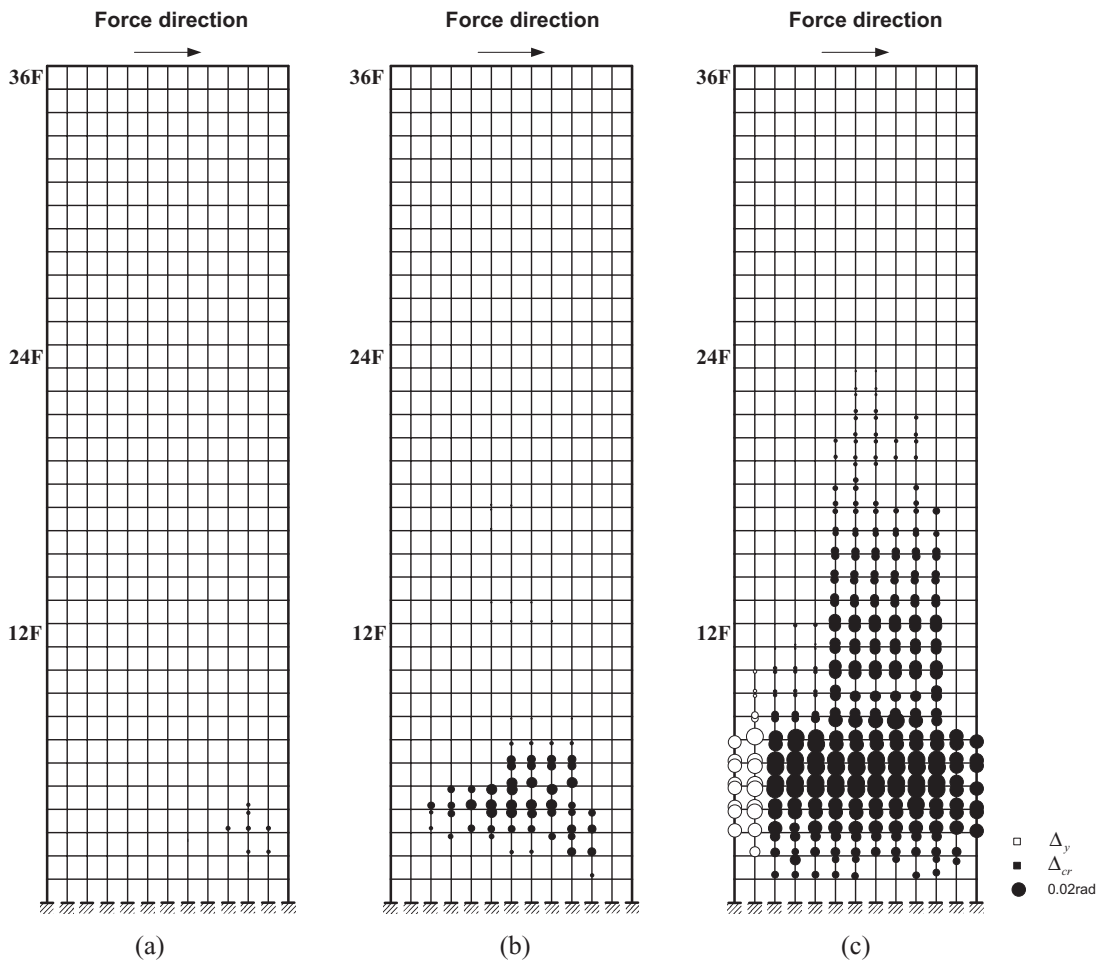

Figure 8. Plastic hinge formation in the web-side frame of the 36-story framed tube structure: (a) at first yield ($\delta_I = 0{\cdot}52\%$); (b) at system yield ($\delta_I = 0{\cdot}54\%$); (c) at $\delta_I = 2\%$

Figure 12 depicts the distribution of inelastic deformation in the web-side frames of the 72-story model structures when the maximum inter-story drifts reached 2% of the story height. Most of the plastic hinges in the 72-story FTS formed in the mid- to high-story columns, which is quite different from the plastic hinge formation in the 36-story FTS, in which plastic hinges formed concentrated in lower-story columns. In the 72-story BTS all braces in the third to 12th stories buckled or yielded and the right-hand-side corner columns buckled under the combined force of bending and compression. As the plastic deformation is focused on a limited number of members, the structure has little ductility, as can be observed in the pushover curves (Figure 7b). Conversely, the plastic deformation in the 72-story BRBTS spread widely throughout the building height, which results in a very large ductility against lateral load. The analysis results imply that by preventing localized damage in the perimeter frames the ductility of tubular structures can be improved significantly. The use of BRB on the surface of tubular structures turned out to be quite effective for this purpose.

Figures 13–15 depict the deformation shapes of the model structures subjected to lateral seismic loads. It can be noticed in Figures 13 and 14 that at the elastic stage (at first yield) both the 36-story

DOI: 10.1002/tal

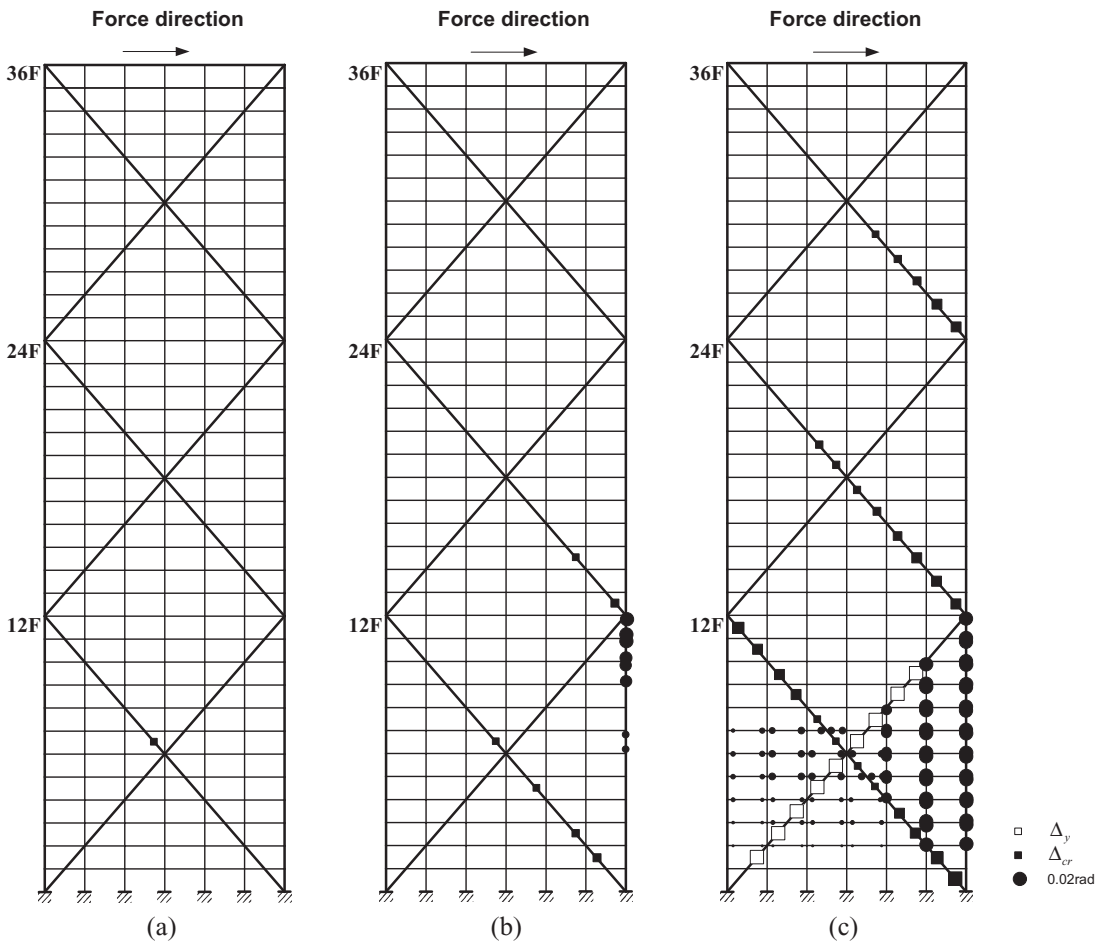

Figure 9. Plastic hinge formation in the web-side frame of the 36-story braced tube structure: (a) at first yield ($\delta_I = 0{\cdot}49\%$); (b) at system yield ($\delta_I = 0{\cdot}59\%$); (c) at $\delta_I = 2\%$

framed and braced tube structures deformed linearly or like cantilever beams. At the maximum inter-story drift of 2%, at which significant inelastic deformation occurred in lower story columns and braces, the structures deformed in shear beam mode. On the other hand, all the 72-story structures deformed in cantilever mode at the maximum inter-story drift of 2%, as shown in Figure 15.

4. BEHAVIOR FACTORS OF TUBE STRUCTURES

Figure 16 represents the typical base-shear versus roof displacement relation of a structure, which can be developed by a nonlinear static pushover analysis. From the figure, the overstrength factor and the ductility factor are defined as follows (Osteraas, 1990):

$$R_o = \frac{V_y}{V_d}, \quad R_\mu = \frac{V_e}{V_y} \tag{4a, b}$$

DOI: 10.1002/tal

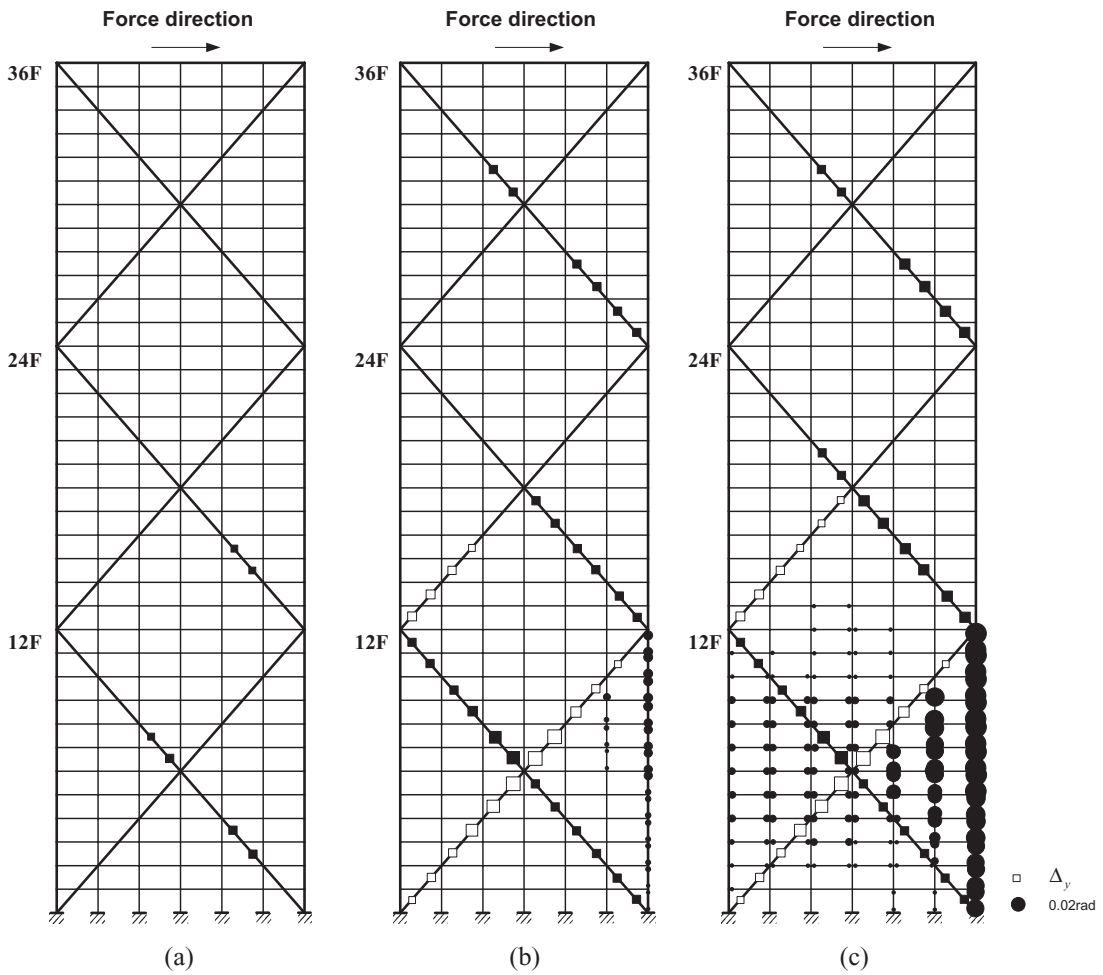

Figure 10. Plastic hinge formation in the web-side frame of the 36-story braced tube structure with BRB: (a) at first yield ($\delta_I = 0{\cdot}27\%$); (b) at system yield ($\delta_I = 0{\cdot}64\%$); (c) at $\delta_I = 2\%$

where V_d is the design base shear, V_e is the maximum seismic demand for elastic response, and V_y is the base shear at yield. FEMA-369 (BSSC, 2001) specified three components of overstrength factors in Table C5.2.7-1: design overstrength, material overstrength, and system overstrength. The ductility factor R_μ is obtained from the system ductility ratio using the procedure proposed by Newmark and Hall (1982), who proposed the following equations for the system ductility factors:

$$\begin{aligned} R_\mu &= 1.0 \; (T < 0{\cdot}03\text{s}) \\ R_\mu &= \sqrt{2\mu - 1} \; (0{\cdot}12 < T < 0{\cdot}5\text{s}) \\ R_\mu &= \mu \; (T > 1{\cdot}0\text{s}) \end{aligned} \tag{5}$$

where T is the natural period of the structure.

The capacity envelopes obtained from pushover analysis (Figure 7) were utilized to evaluate overstrength and ductility factors. Figure 17(a) shows the overstrength factors of the model structures, in

DOI: 10.1002/tal

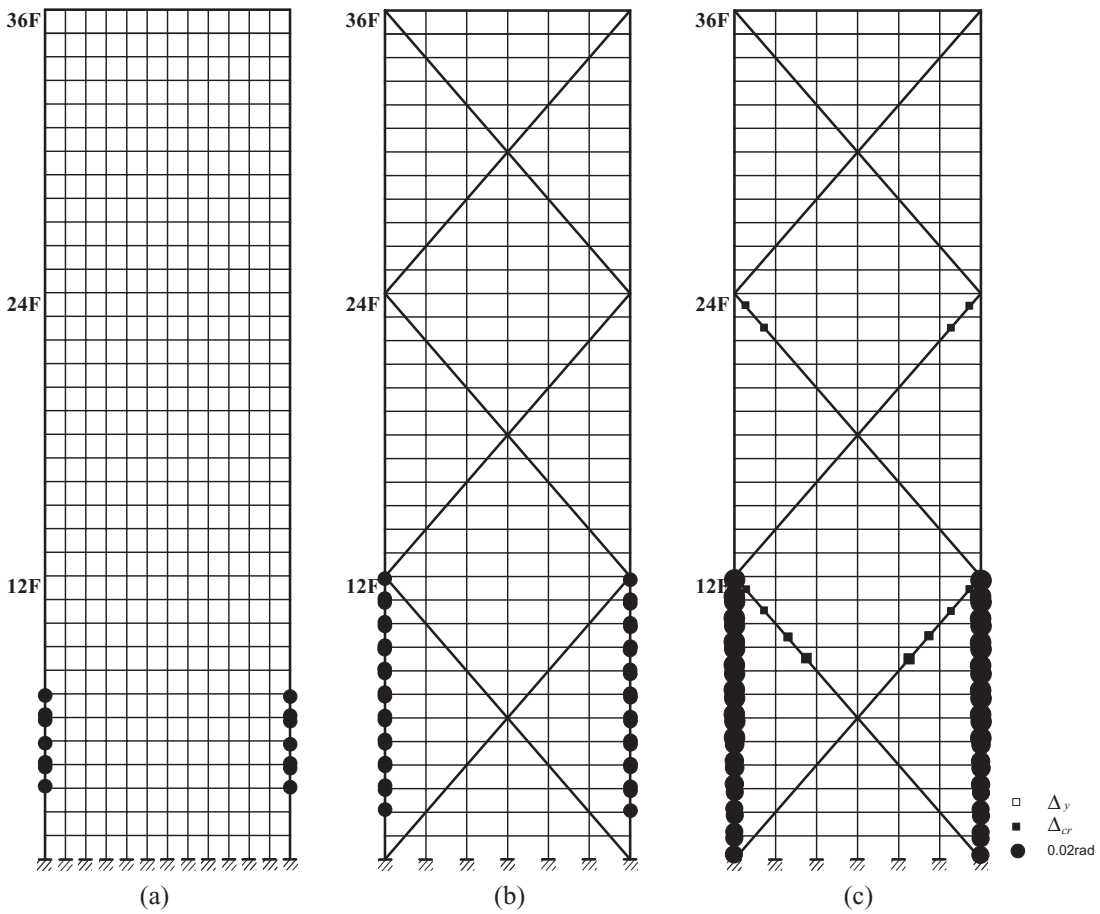

Figure 11. Plastic hinge formation in the flange-side frame of the 36-story model structures at the maximum inter-story drift of 2%: (a) FTS; (b) BTS; (c) BRBTS

which it can be observed that the model structures with tubular system have higher overstrength than observed in typical low-rise buildings. It also can be observed that the 72-story structures retain larger overstrength than the 36-story structures. In general, the overstrength factor increases as the number of stories decreases because the effect of seismic load is more significant compared to the effect of gravity load in low-rise structures. In this study, however, the design wind load was significantly larger than the seismic load and the member size initially designed for strength was further increased to meet the displacement limit state for wind load, which resulted in larger overstrength factors in the 72-story analysis model structures. It should also be pointed out that the overstrengths of tall buildings depend on drift criteria for wind load. Therefore, if a stricter drift criterion is applied, the overstrength will increase. It can be observed in the figure that the overstrength of structures with braces was significantly larger than that of the FTS, which results from the inherent effectiveness of braced frames in resisting lateral load. The overstrength of BRBTS turned out to be a little larger than that of the BTS. Figure 17(b) plots the ductility factor of the model structures, which is the maximum displacement at stable state divided by the system level yield displacement. Figure 12(b) shows that the inelastic

DOI: 10.1002/tal

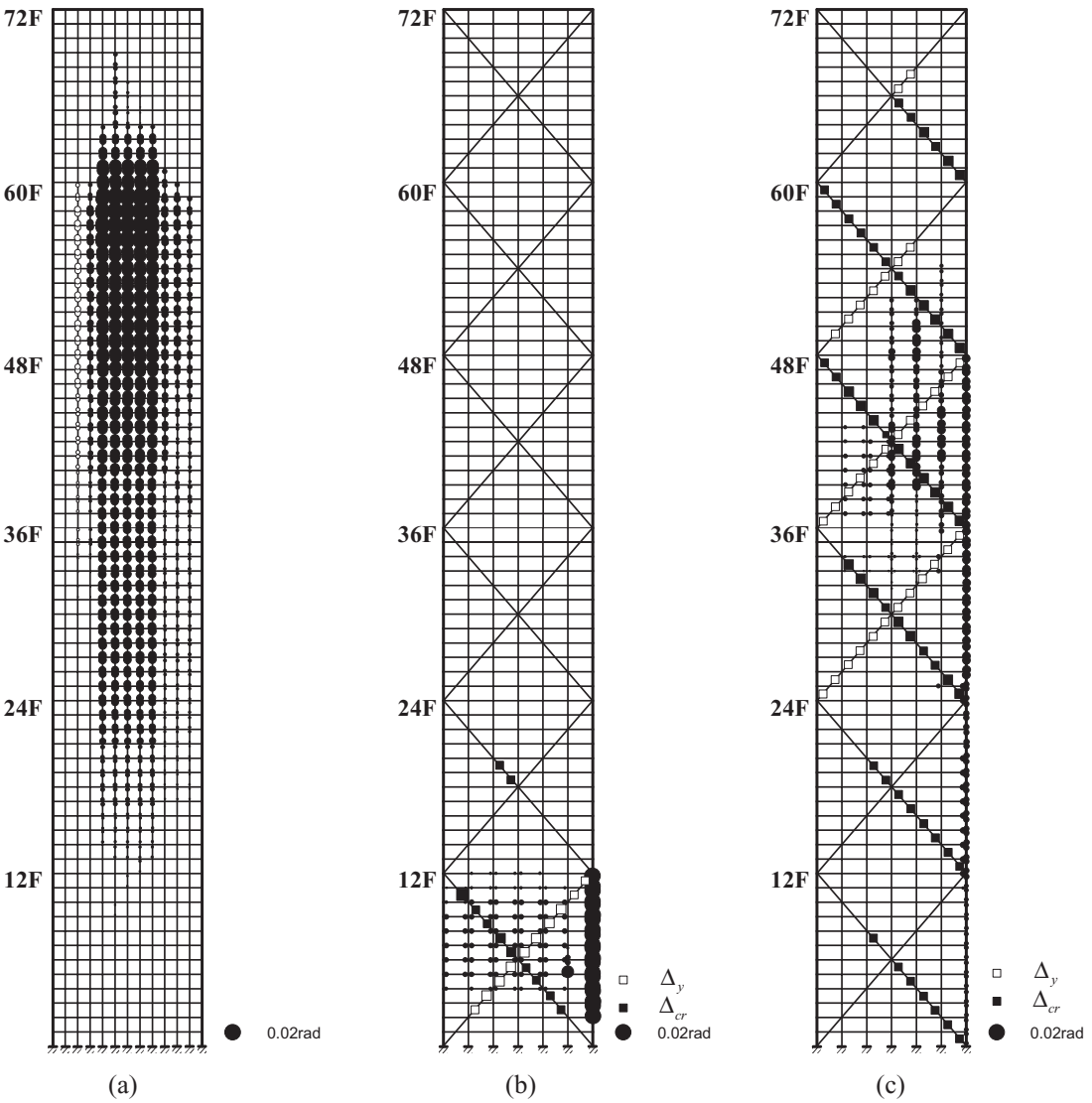

Figure 12. Plastic hinge formation in the web-side frame of the 72-story tube structures: (a) FTS; (b) BTS; (c) BRBTS

deformation (mostly buckling of columns and braces) in the 72-story BTS is highly concentrated in the lower stories, which results in a small ductility factor and brittle failure mode. The ductility factors of the framed tube structures are slightly larger than those of the other structures, and the ductility factors of the BRBTS are larger than those of the BTS. In all cases the ductility factors of the 72-story structures are smaller than those of the 36-story structures.

The response modification factors were computed by multiplying the overstrength and the ductility factors as recommended by ATC-19 (1995). Figure 17(c) shows the response modification factors of the model structures, where it can be observed that the factors for the model structures, which range

DOI: 10.1002/tal

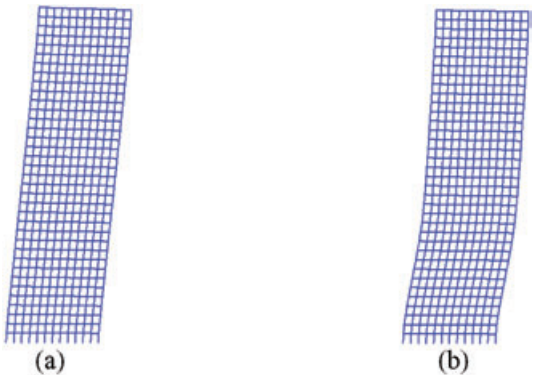

Figure 13. Deformation shape of the 36-story framed tube structure (scale factor: 2): (a) at first yield; (b) at inter-story drift of 2%

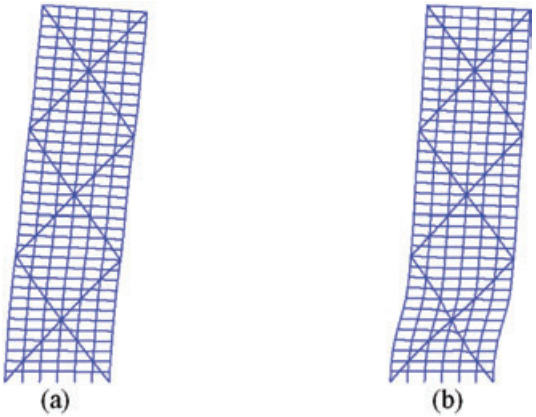

Figure 14. Deformation shape of the 36-story braced tube structure (scale factor: 2): (a) at first yield; (b) at inter-story drift of 2%

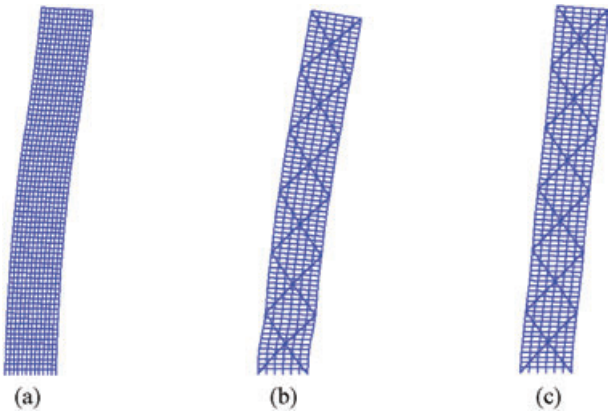

Figure 15. Deformation shape of the 72-story tube structures (scale factor: 2): (a) FTS; (b) BTS; (c) BRBTS

DOI: 10.1002/tal

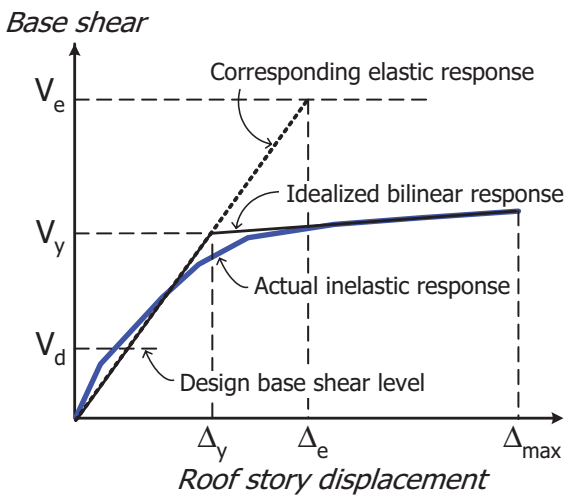

Figure 16. Idealized base shear–roof displacement relationship of a structure

from 10·5 to 14·5, are significantly larger than the design response modification factor used in this study, which is 3·0. Even though a large part of the factors is contributed from the overstrength rather than from the ductility capacity of the structures, the tubular structures retain a superior seismic load-resisting capacity; the BRBTS in particular showed the largest *R*-factors.

5. NONLINEAR DYNAMIC ANALYSIS RESULTS

It is well documented in the literature that nonlinear static analysis may not properly predict the dynamic behavior of tall buildings in which participation of higher modes is significant. In this section nonlinear dynamic time-history analyses were carried out using SAP 2000 with the three earthquake records shown in Figure 18: El Centro earthquake (NS) and the two earthquakes developed for the SAC Steel Project, LA29 and LA30 (Somerville *et al.*, 1997). Figure 19 shows the location and magnitude of plastic hinges formed in the 36-story framed tube structure (web-side) by input of three different levels of the El Centro earthquake. It can be noticed that plastic hinges formed first at upper stories with the El Centro earthquake with peak ground acceleration (PGA) equal to 0·357 *g*, and spread to lower stories as the intensity of the earthquake increased. The analysis results of the other earthquake records were similar to those shown in the figure. This is quite different from the sequence of plastic hinge formation predicted by pushover analysis shown in Figure 8, in which the plastic hinges formed in lower stories and spread upward up to the mid-height of the structure.

Figure 20 compares the base shear–roof displacement relationship of the 36-story framed tube structure obtained from pushover analysis and from incremental dynamic analysis using the three earthquake records. The incremental dynamic analyses were carried out by gradually increasing the PGA of the records. It can be seen that the initial stiffness of the structure predicted by the static and dynamic analyses matches well with each other. It can also be observed that the pushover curve forms the lower bound of those obtained by incremental dynamic analysis. This is quite reasonable considering the fact that the inelastic deformation is concentrated in the lower stories in static pushover analysis, whereas in dynamic analysis the plastic hinges are more widely distributed throughout the structure, contributing to higher strength and ductility.

DOI: 10.1002/tal

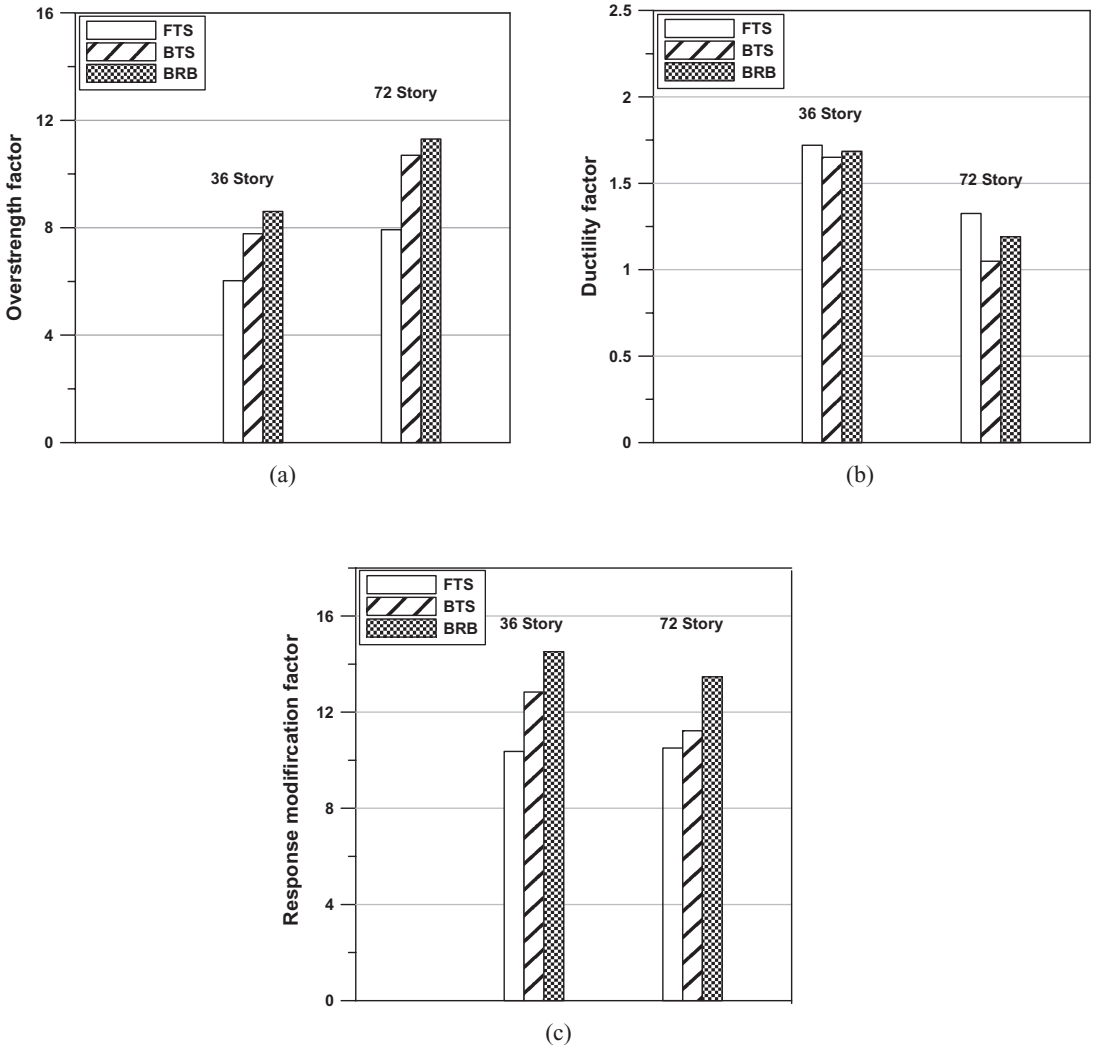

Figure 17. Behavior factors of the model structures: (a) overstrength factors; (b) ductility factors; (c) response modification factors

The above results indicate that there exist discrepancies between nonlinear static and dynamic analysis results in high-rise tubular structures. However, it was confirmed that the load–displacement relationship estimated by static pushover analysis formed the lower bound of the dynamic analysis results. Therefore behavior factors such as the overstrength, ductility, and response modification factors obtained based on the static pushover curve are conservative values and can safely be used for seismic design.

DOI: 10.1002/tal

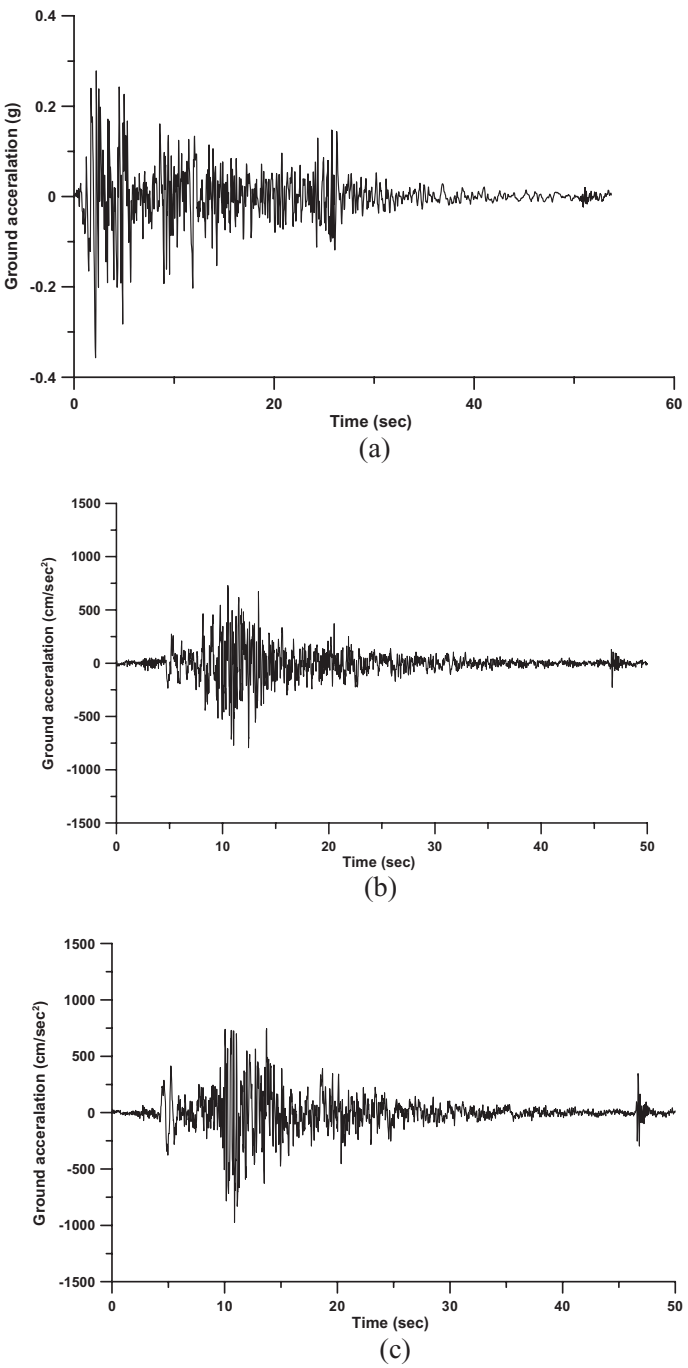

Figure 18. Earthquake records used in the dynamic time-history analysis: (a) El Centro earthquake (NS components); (b) LA 29 record; (c) LA 30 record

DOI: 10.1002/tal

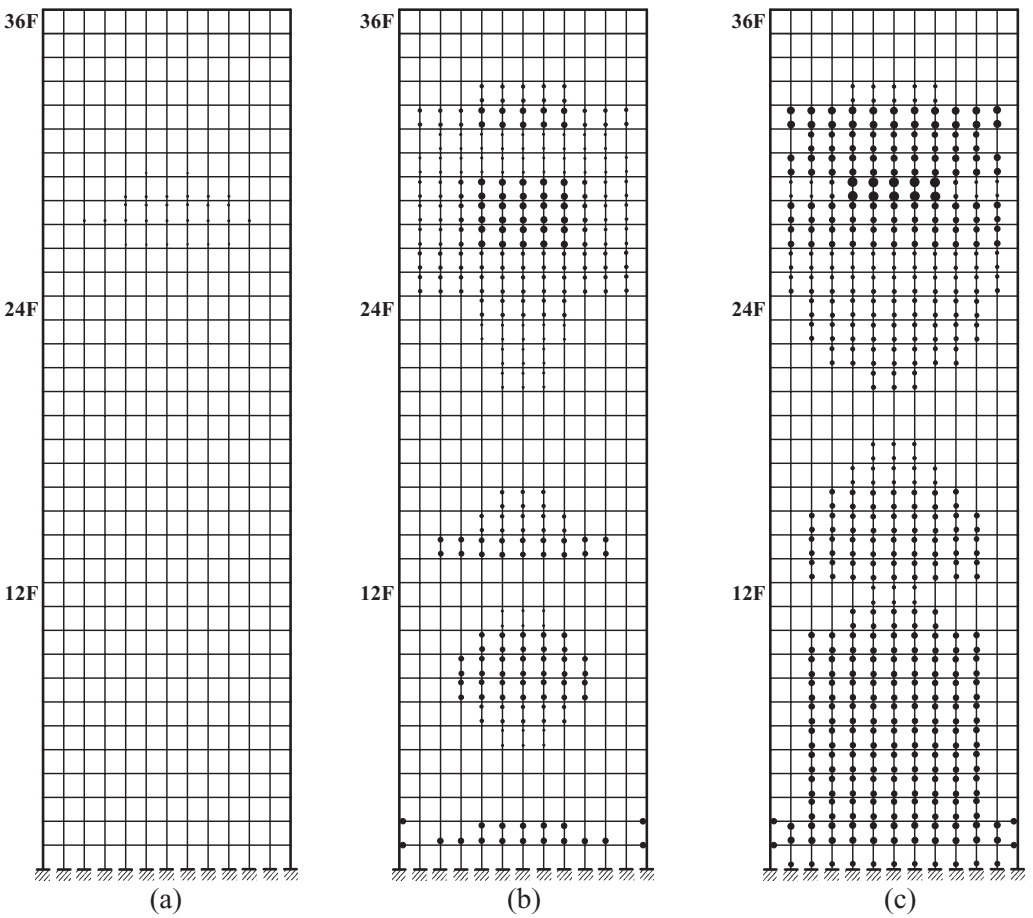

Figure 19. Plastic hinges formed in the 36-story framed tube structure (web-side) obtained by dynamic time-history analysis using the El Centro earthquake records (NS) with three levels of peak ground accelerations: (a) PGA = 0·357 *g*; (b) PGA = 0·7 *g*; (c) PGA = 0·8 *g*

6. CONCLUSIONS

In this study 36- and 72-story framed and braced tubular structures were designed according to the current design code and their seismic performance was evaluated by nonlinear static and dynamic analysis. According to the analysis results, the tubular structures generally showed high earthquake-resisting capability. The framed tube structures showed lower stiffness and strength compared with tube structures with diagonal braces. The braced tube structures showed greater strength but lower overall ductility compared with framed tube structures. When buckling-restrained braces were used instead of conventional braces, strength increased significantly compared with the framed tube, and ductility was enhanced compared with braced tube structures. The load–displacement relationship estimated by static pushover analysis formed the lower bound of the dynamic analysis results. The response modification factors obtained from pushover analysis ranged from about 10 to 14, which is significantly higher than the code-specified values normally used for seismic design of structures.

DOI: 10.1002/tal

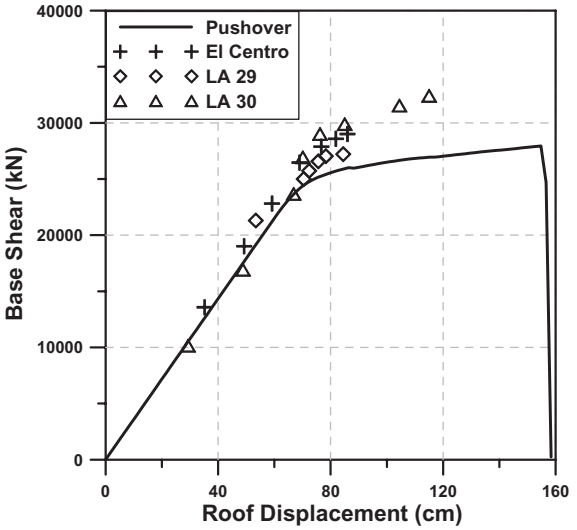

Figure 20. Comparison of base shear–roof displacement relationship of the 36-story framed tube structure obtained from pushover analysis and incremental dynamic analysis

ACKNOWLEDGEMENTS

This work was supported by the Basic Research Program of the Korea Science and Engineering Foundation (grant no. M10600000234-06J0000-23410) and the SRC/ERC program of MOST/KOSEF (R11-2005-056-01003-0). The authors appreciate this financial support.

REFERENCES

AISC LRFD. 2000. *Load and Resistance Factor Design Specification for Structural Steel Buildings*. American Institute of Steel Construction: Chicago.

AISC. 2005. *Seismic Provisions for Structural Steel Buildings*. American Institute of Steel Construction: Chicago, IL.

ATC-19. 1995. *Structural Response Modification Factors*. Applied Technology Council: Redwood City, CA.

Black C, Makris N, Aiken I. 2001. *Component Testing, Stability Analysis and Characterization of Buckling Restrained Braces*. Final report to Nippon Steel Corporation: Tokyo.

BSSC. 2001. NEHRP: *Recommended Provisions for Seismic Regulations for New Buildings and Other Structures*. Part 2: *Commentary*. FEMA-369. Building Seismic Safety Council: Washington, DC.

BSSC. 2004. NEHRP *Recommended Provisions for Seismic Regulations for New Buildings and Other Structures*. Part 1: *Provisions*. FEMA-450. Building Seismic Safety Council: Washington, DC.

Connor JJ, Pouangaree CC. 1992. Simple model for design of framed-tube structures. *Journal of Structural Engineering, ASCE* **117**(12): 3623–3643.

Freeman S, Sasaki K, Paret T. 1998. Multi-mode push-over procedure (MMP). In *Proceedings of the 6th National Conference on Earthquake Engineering*. EERI, Seattle, WA.

ICC. 2006. *International Building Code*. International Code Council: Washington, DC.

Koran AKH. 1994. Simple method for approximate analysis of framed tube structures. *Journal of Structural Engineering* **120**(4): 1221–1239.

MIDAS. 2007. Genw. *General Structure Design System for Windows*. MIDAS IT Seoul, Korea.

Newmark NM, Hall WJ. 1982. *Earthquake Spectra and Design*. EERI Monograph Series. Earthquake Engineering Research Institute: Oakland, CA.

DOI: 10.1002/tal

Osteraas JD. 1990. Strength and ductility considerations in seismic design. PhD dissertation, Stanford University, Stanford, CA.

Somerville P, Smith H, Puriyamurthala S, Sun J. 1997. *Development of Ground Motion Time Histories for Phase 2 of the FEMA/SAC Steel Project*. SAC/BD 97/04. Sacramento, CA.

Taranath BS. 1998. *Steel, Concrete, and Composite Design of Tall Buildings*. McGraw-Hill: New York.

Tremblay R, Degrange D, Blouin J. 1999. Seismic rehabilitation of a four-story building with a stiffened bracing system. In *Proceedings of the 8th Canadian Conference on Earthquake Engineering*, Vancouver, 1999.

DOI: 10.1002/tal